energies

MDPI

Article

Second-Order Sliding Mode Control of Permanent Magnet Synchronous Motor Based on Singular Perturbation

Zhiming Liao [1,*], Yue Hao [2], Tao Guo [2], Bingxin Lv [2] and Qiang Wang [2]

[1] National Maglev Transportation Engineering R&D Center, Tongji University, Shanghai 200092, China
[2] School of Electrical Engineering, China University of Mining and Technology, Xuzhou 221116, China
* Correspondence: liaozhiming@tongji.edu.cn

Abstract: The second-order sliding mode control has strong robustness. Its application has greatly improved the anti-jamming ability of permanent magnet synchronous motor(PMSM) speed control systems. However, the influence of noise is unavoidable due to the introduction of a differentiator in the second-order sliding mode control, and the steady-state performance of the system is poor due to the absence of a q-axis current loop. This paper proposes a second-order sliding mode control method based on singular perturbation, which decouples the PMSM speed control system into two subsystems, the slow subsystem, including the speed variable, adopts second-order sliding mode control, and the fast subsystem, including the current variable of q-axis, adopts linear control. The design of a sliding surface for the slow subsystem avoids the application of the differentiator, which reduces the chattering better. Besides this, the steady-state performance of the system is improved due to the introduction of the feedback current of the q-axis. Experimental results show that the proposed method has strong robustness and can achieve high-precision control.

Keywords: permanent magnet synchronous motor; second-order sliding mode control; singular perturbation

Citation: Liao, Z.; Hao, Y.; Guo, T.; Lv, B.; Wang, Q. Second-Order Sliding Mode Control of Permanent Magnet Synchronous Motor Based on Singular Perturbation. *Energies* **2022**, *15*, 8028. https://doi.org/10.3390/en15218028

Academic Editor: Hui Zhang

Received: 22 September 2022
Accepted: 25 October 2022
Published: 28 October 2022

1. Introduction

A permanent magnet synchronous motor (PMSM) has the advantages of high operating efficiency, high power density, and high starting torque. They are widely used in modern industrial fields and are of great significance for improving the efficiency of electric energy utilization and achieving energy saving and emission reduction [1]. However, the PMSM system is a multi-variable, strongly coupled, and nonlinear system. There are many challenges in the design of its control system. In order to achieve efficient control of PMSM, many control algorithms have been proposed and applied to the control of PMSM, such as proportional integral (PI) control based on fractional order [2], intelligent PI control [3,4], model Predictive control [5], adaptive control [6], and sliding mode control (SMC) [7], etc. Applying sliding mode control, only the parameters of the controlled system and the change interval of system disturbances need to be determined. The control law is designed to make the system operate on a sliding surface to obtain a good control effect. The control algorithm has strong robustness, fast dynamic response, and easy implementation. Therefore, the study of the application of sliding mode control in the PMSM speed control system has great significance.

The American scholar K.D. Young studied the impact of chattering on the system in the practical application of sliding mode control and proposed several methods that can be applied to the practical system to reduce the chattering [7]. Wang et al. [8] present a new integral sliding mode control method for fuzzy stochastic systems subjected to matched/mismatched uncertainties. A novel fuzzy integral sliding manifold function is adopted such that the matched uncertainties are completely rejected while the mismatched ones will not be enlarged during the sliding mode phase. A fuzzy sliding mode controller is

further presented to maintain the states of the fuzzy stochastic system onto the predefined fuzzy manifold in the presence of uncertainties. In [9], a new sliding mode control design methodology for fuzzy singularly perturbed systems subject to matched/unmatched uncertainties is presented. A novel integral-type fuzzy switching surface function is put forward. A modified adaptive fuzzy SMC law is further constructed for adapting the unknown upper bound of the matched uncertainty.

In [10], The term terminal switch gain is added to the law of exponential approximation, and the saturation function replaces the traditional switch function. In [11], A discrete-time fractional-order variable structure terminal sliding mode linear motor speed controller is designed by combining fractional order control and sliding mode control, and the dynamic performance of the motor speed has been improved. In [12], by combining the backstepping control and the sliding mode control, the fault-tolerant control of the manipulator will have the advantages of strong robustness, fast transient response, and limited convergence time. Furthermore, it has an asymptotically stable backstepping control Strategy globally. In [13], in order to optimize the dynamic performance of the PMSM nonlinear speed regulation system, a new reaching law is designed, and the problem of large chattering caused by high switching gain is considered. An extended state observer is introduced to observe the total disturbance, and a feedforward compensation is used when the disturbance is observed. In [14], a sliding mode controller based on model reference adaptive control (MRAC) is proposed for PMSM systems. This strategy can reduce the complexity of MRAC identification so that the response of the PMSM system is consistent with the reference model to reduce the influence of uncertain system parameters and load disturbance. In [15], a sliding mode observer is used in the control algorithm of position sensorless for PMSM, which can reduce the estimation error of position in a wider speed range and has higher accuracy. In [16], a robust model-free nonsingular terminal sliding-mode control based on the super-local model is proposed to reduce the influence of demagnetization of PMSM. It not only maintains the robustness of the PMSM drive system but also improves the system's dynamic response, reduces the dependence of controller design for accurate models, and has the function of fault tolerance and demagnetization. In [17], by the Lyapunov function, a second-order sliding mode control system is designed to realize the speed control of the PMSM, which greatly improves the control system's dynamic performance and parameter robustness.

In [18], a synchronous reluctance motor vector controller based on second-order sliding mode control is built. It is suitable when the mechanical load often changes. In [19], a first-order and second-order hybrid sliding mode control system is proposed for the chattering phenomenon of the PMSM servo drive system, and the parameters of the hybrid sliding mode control system are tuned by using fuzzy logic inference system. It not only improves the accuracy of the system's parameters in practical applications but also enhances the anti-disturbance capability of the system. In [20], a second-order sliding mode control strategy based on multiple inputs and outputs is proposed for the common parameter uncertain and large load disturbance in practical applications, which can make the controller converge and achieve the desired control effect in the conditions of parameters uncertain and output coupling. In [21], a compound control strategy is achieved for chatter-free speed regulation by approximating the relationship between q-axis reference current and speed as a second-order model and using a continuous sliding mode controller. It introduces a disturbance observer as a compensator to reduce the influence of disturbance and get a good control effect. In [22], a discrete-time super-twisting sliding mode (DTSTSM) current controller for switched reluctance motors is proposed. The method uses a cost function that allows the controller's gain to be adjusted online according to the rotor speed. The application of the proposed method does not require knowledge of motor parameters, and the method also uses a pulse-width modulation technique to ensure a fixed switching frequency. In [23], a model-free control using improved smoothing extended state observer and super-twisting nonlinear sliding mode control for PMSM drives is proposed. The proposed method uses an improved smoothing extended state observer to estimate the unknown parameters

of the motor model. The nonlinear sliding mode surface is designed, can overcome the disadvantages of conventional linear sliding mode surface. Meanwhile, a super twist structure is chosen to improve the system's robustness. In [24], a hermit neural network-based second-order sliding-mode control of synchronous reluctance motor drive systems is proposed. The controller consists of a compound speed control loop and a compound current control loop. The designed controller achieves tracking control of rotor angular speed and compensates for disturbances and errors.

The classic super-twisting algorithm-based second-order sliding-mode controller is challenging to design. Six parameters need to be confirmed, and they are related to the uncertainty bound of the system. If considering limiting the output signal, it will change the parameter values. Moreover, its stability analysis is complex. In order to avoid the design of complex robust differentiators, a second-order sliding mode control strategy for PMSM based on a super-twisting algorithm is proposed. This controller decomposes the system into two reduced-order subsystems by singular ingestion, designs independent controllers respectively, and obtains the final controller after superimposing the two controllers. In this controller, only four parameters need to be considered, further simplifying the design process of the second-order sliding mode control. High-frequency noise generation can be avoided due to the omission of the robust differentiator. Their stability is determined by having negative real parts for all the eigenvalues of the state variable coefficient matrices in both subsystems, and the stability of both subsystems ensures the stability of the entire control system.

The main contributions of this article can be summarized as follows.

(1) A new second-order sliding mode control strategy for PMSM based on a super-twisting algorithm is proposed. The proposed controller requires fewer parameters to be determined, presenting a simple design structure and excellent performance.
(2) The adopted singular regimens theory decomposes the speed control link into fast and slow subsystems for control. The stability analysis is determined by the eigenvalues of the state variable coefficient matrices in the two subsystems.
(3) The control performance is compared with the conventional second-order superhelix sliding mode controller, showing better dynamic and static performance.

2. Mathematical Model of PMSM

The mathematical model of PMSM in the d-q coordinate system. The voltage state equation of PMSM in the d-q coordinate system is shown below.

$$\begin{cases} u_{\mathrm{d}} = R_{\mathrm{s}} i_{\mathrm{d}} + \frac{\mathrm{d}\psi_d}{\mathrm{d}t} - \omega_{\mathrm{e}} \psi_q \\ u_q = R_{\mathrm{s}} i_q + \frac{\mathrm{d}\psi_q}{\mathrm{d}t} + \omega_{\mathrm{e}} \psi_d \end{cases} \tag{1}$$

In (1), R_{s}, u_{d}, u_{q}, i_{d}, i_{q}, ψ_{d}, ψ_{q} are the stator resistance, stator voltage, stator current, and stator flux linkage in the d-q coordinate system, respectively.

The stator flux linkage equation of PMSM is written as:

$$\begin{cases} \psi_{\mathrm{d}} = L_{\mathrm{d}} i_{\mathrm{d}} + \psi_{\mathrm{f}} \\ \psi_q = L_q i_q \end{cases} \tag{2}$$

In (2), L_{d} and L_{q} are the inductance components of the d-q axes, respectively. Ψ_{f} is the permanent magnet flux linkage.

The electromagnetic torque equation of PMSM can be expressed as:

$$T_{\mathrm{e}} = \frac{3}{2} p_{\mathrm{n}} \left(\psi_{\mathrm{f}} + \left(L_{\mathrm{d}} - L_{\mathrm{q}} \right) i_{\mathrm{d}} \right) i_{\mathrm{q}} \tag{3}$$

In (3), p_{n} is the pole pairs.

When the motor is a Permanent Surface Magnet Synchronous Motor (SPMSM), $L_d = L_q = L$. Equation (3) can be transformed as:

$$T_e = \frac{3}{2} p_n \psi_f i_q \tag{4}$$

3. Second-Order Sliding Mode Control

This paper takes $i_d = 0$ control strategy. i_d can be omitted. Since a hidden pole permanent magnet synchronous motor is selected in this paper. So there is no reluctance torque. The state equation of PMSM can be simplified as follows:

$$\begin{cases} \frac{d\omega_r}{dt} = \frac{1}{J}[\frac{3}{2} {p_n}^2 \psi_f i_q - p_n T_L - B\omega_r] \\ \frac{di_q}{dt} = \frac{1}{L_q}(-R_s i_q + u_q) \end{cases} \tag{5}$$

In order to simplify the calculation of the derivatives of the sliding surface, the items in (5) are replaced with other symbols, and the following formula is obtained:

$$\begin{cases} \dot{x}_1 = k_1 x_1 + k_2 x_2 + k_3 \\ \dot{x}_2 = k_4 x_2 + k_5 u \end{cases} \tag{6}$$

In (6), $x_1 = \omega_r$, $x_2 = i_q$, $u = u_q$, $k_1 = -B/J$, $k_2 = 3p_n^2 \psi_f i_q / J$,$k_3 = -p_n T_L / J$,$k_4 = -R_s i_q / L_q$,$k_5 = 1/L_q$. Take the given desired speed as ω_r^*, the speed error is $e = \omega_r^* - \omega_r$, take the sliding surface as $s = c_1 e + c_2 \dot{e}$, $c_1 > 0$ and $c_2 > 0$, the system convergence speed can speed up by increasing the value. Since these two coefficients reflect the speed and the acceleration of the speed about the weight of the distance error of the sliding surface when selecting the values, it is necessary to follow a suitable ratio to ensure that both the speed and the acceleration of the speed have the influence on the sliding surface. If one of them is too large or too small, other items' influence on the sliding surface's distance error is not annihilated or has an absolute effect.

Expand the sliding surface s and $\dot{s}$, $\ddot{s}$, can get:

$$\begin{aligned} s &= c_1(x_1 - x_1^*) + c_2(\dot{x}_1 - \dot{x}_1^*) \\ &= (c_1 + c_2 k_1)x_1 + c_2 k_2 x_2 - c_1 x_1^* - c_2 \dot{x}_1^* + c_2 k_3 \end{aligned} \tag{7}$$

$$\begin{aligned} \dot{s} = (c_1 k_1 + c_2 k_1^2)x_1 + (c_1 k_2 + c_2 k_1 k_2 + c_2 k_2 k_4)x_2 \\ + c_2 k_2 k_5 u + (c_1 + c_2 k_1)k_3 - c_1 \dot{x}_1^* - c_2 \ddot{x}_1^* \end{aligned} \tag{8}$$

Take $k_6 = c_1 k_1 + c_2 k_1^2$,$k_7 = c_1 k_2 + c_2 k_1 k_2 + c_2 k_2 k_4$, the above formula (8) can be equivalent to:

$$\begin{aligned} \dot{s} = k_6 x_1 + k_7 x_2 + c_2 k_2 k_5 u + (c_1 + c_2 k_1)k_3 \\ - c_1 \dot{x}_1^* - c_2 \ddot{x}_1^* \end{aligned} \tag{9}$$

$$\begin{aligned} \ddot{s} = k_6 k_1 x_1 + (k_6 k_2 + k_7 k_4)x_2 + k_6 k_3 + k_7 k_5 u \\ - c_1 \ddot{x}_1^* - c_2 \dddot{x}_1^* + c_2 k_2 k_5 \dot{u} \end{aligned} \tag{10}$$

Take $\varphi = k_6 k_1 x_1 + (k_6 k_2 + k_7 k_4)x_2 + k_6 k_3 + k_7 k_5 u - c_1 \ddot{x}_1^* - c_2 \dddot{x}_1^*$, $\gamma = c_2 k_2 k_5$, the above formula (10) can be equivalent to:

$$\ddot{s} = \varphi + \gamma \dot{u} \tag{11}$$

Assuming $-A \le \varphi \le A, A \ge 0$, $0 < B_m \le \gamma \le B_M$, let $v = \dot{u}$, the problem of second-order sliding mode control can be equivalent to the finite-time stability problem of the nonlinear system shown as follows:

$$\begin{cases} y_1 = s \\ \dot{y}_1 = y_2 \\ \dot{y}_2 = \varphi + \gamma v \end{cases} \tag{12}$$

The u consists of two parts:

$$\begin{cases} u = u_1 + u_2 \\ u_1 = -m_1|s|^{\frac{1}{2}}\mathrm{sgn}(s) \\ \dot{u}_2 = -m_2\mathrm{sgn}(s) \end{cases} \tag{13}$$

when m_1 and m_2 satisfy the following formula, the system will converge.

$$\begin{cases} m_1^2 \geq \frac{4AB_M(m_2+A)}{B_m^3(m_2-A)} \\ m_2 > \frac{A}{B_m} \end{cases} \tag{14}$$

Since the variable of the sliding mode surface designed in this paper contains the first derivative of the speed, it cannot be directly measured. If it is obtained by directly taking the derivative of the speed, the result will be distorted due to the high-frequency noise contained in the speed, and the high-frequency noise needs to be removed, but if a low-pass filter filters out the high-frequency noise, it will bring about the problem of phase lag. Therefore, it is necessary to design a differential observer to measure the acceleration of the speed. At present, the common differential observers are not sensitive to high-frequency signals and consider them noise. However, in the process of removing noise, it is difficult to avoid that the non-noise signal is not affected, and it will also be filtered out. It is necessary to use the sliding mode algorithm to design the differential observer when the compositions of a given signal are uncertain. The traditional sliding mode observer has the problem of chattering. In order to overcome the problem and make the differential observer strong robustness, this paper adopts a robust differentiator of the second-order sliding mode based on the super-twisting algorithm. The schematic diagram is shown in Figure 1:

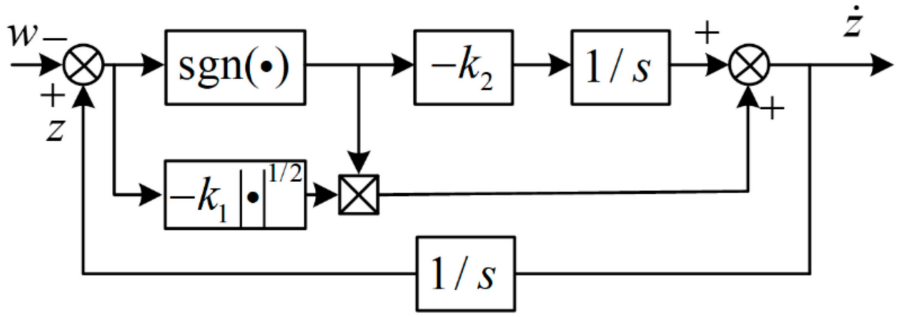

Figure 1. Schematic diagram of the robust differentiator.

Take the sliding mode surface of the robust differentiator:

$$s = z - \omega_\mathrm{r} \tag{15}$$

In (15), z is the observed speed, ω_r is the actual speed. Using the control law shown in (13), taking $z(0) = \omega_\mathrm{r}(0) = 0$, selecting the control parameters according to equation (14), finally the system can converge. $u = \dot{z}$ is the observed acceleration.

The schematic diagram of the second-order sliding mode control system is shown in Figure 2:

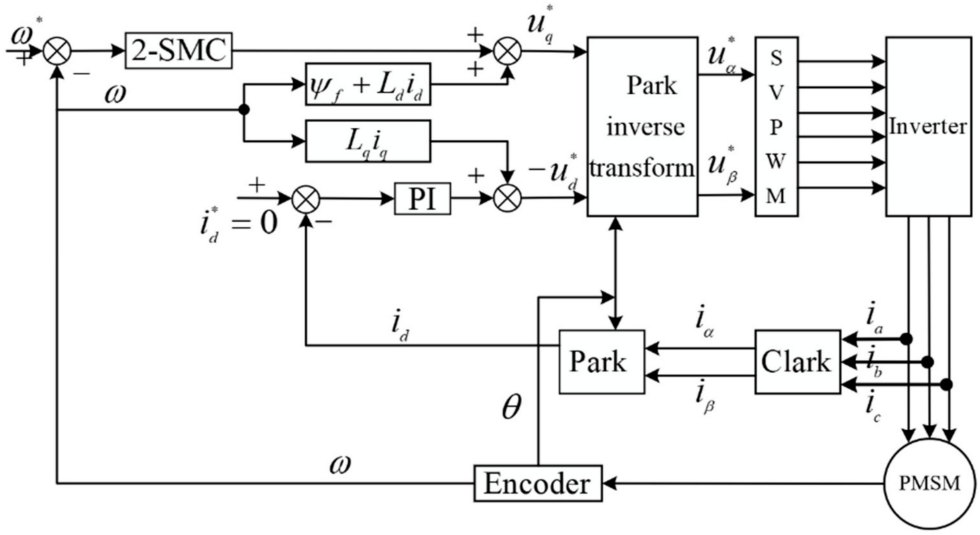

Figure 2. Schematic diagram of second-order sliding mode control of PMSM.

For the second-order sliding mode control of PMSM, it is still necessary to design a robust differentiator to obtain the derivative estimation of the speed when super-twisting control with the least information is used. In order to further simplify the design and avoid the high-frequency noise caused by the application of the differentiator, the system is decomposed into two reduced-order subsystems by means of singular perturbation, and independent controllers are designed for the two subsystems, the control laws of the two controllers are added together to obtain a composite control, which further simplifies the design of the second-order sliding mode control and reduces the high-frequency noise caused by the differentiator:

4. Second-Order Sliding Mode Control Based on Singular Perturbation

The PMSM servo system is multi-variable, and the time for variables of different time scales to reach stability varies greatly. When solving the differential equation of state and the selected sampling step size is larger, it will cause a larger error due to the rapid change of the fast variable. Therefore, a smaller sampling step must be adopted. This characteristic is called rigidity. When the ratio of rigidity is much greater than 1, the differential equation is called an ill-posed equation. The singular perturbation method can solve the rigidity problem well caused by the multiple time scales. By decomposing the original system into fast and slow subsystems and designing two controllers respectively, the problem of rigidity is solved approximately, and the controller design of the reduced-order system is easier.

In order to simplify the design of the second-order sliding mode control of the PMSM and avoid the influence of high-frequency noise caused by the robust differentiator, the original system is decomposed and reduced order by using the method of singular perturbation, which removes the speed differential term in the design of the sliding surface and simplifies the design of the sliding surface and avoids the influence of high-frequency noise caused by the robust differentiator. In order to obtain the fast and slow subsystems, the system state equation in (5) is decomposed according to the theory of singular perturbation, and then the controllers are designed, respectively.

4.1. Decoupling of Fast and Slow Subsystems

Transform formula (5) into the system state equation in the form of singular perturbation. Take and get the following formula:

$$\begin{cases} \dot{\omega}_r = \frac{1}{J}[\frac{3}{2}{p_n}^2\psi_f i_q - p_n T_L - B\omega_r] \\ \varepsilon\dot{i}_q = -R_s i_q + u_q \end{cases} \tag{16}$$

Further decoupling Equation (16), let $\varepsilon \to 0$, i_q can be replaced by q-axis stator voltage of slow subsystem, and get the slow subsystem as follows:

$$\dot{\omega}_{rs} = \frac{1}{J}[\frac{3}{2}{p_n}^2 \psi_f \frac{u_{qs}}{R_s} - p_n T_L - B\omega_{rs}] \tag{17}$$

In (17), ω_{rs} is the rotor speed of slow subsystem.

When the fast subsystem changes, it is considered that the slow subsystem variables remain unchanged. The state equation of the fast subsystem can be obtained:

$$\varepsilon \dot{i}_{qf} = -R_s i_{qf} + u_{qf} \tag{18}$$

In (18), i_{qf} is the q-axis stator current of the fast subsystem. u_{qf} is the q-axis stator voltage of the fast subsystem.

For the speed control system of PMSM, the given expected signal is the speed for the q-axis. The actual speed is hoped to be consistent with the expected speed. Therefore, for the slow subsystem that only contains the speed variable, the sliding surface is designed as follows:

$$s = c_1(\omega_{rs} - {\omega_r}^*) \tag{19}$$

Let $-B$=k_1, $-P_n T_L$=$k^{'}_2$, $3p_n^2 \psi_f / 2R_s J = k'_3$, $u_{qs} = u$ can get $\dot{s}$ and $\ddot{s}$:

$$\dot{s} = c_1\dot{\omega}_{rs} - c_1{\dot{\omega}_r}^* = c_1 k'_1 \omega_{rs} + c_1 k'_2 + c_1 k'_3 u - c_1{\omega_r}^* \tag{20}$$

$$\begin{aligned} \ddot{s} &= c_1\ddot{\omega}_{rs} - c_1{\ddot{\omega}_r}^* = c_1 k_1'^2 \omega + c_1 k'_1 k'_2 \\ &+ c_1 k'_1 k'_3 u - c_1{\ddot{\omega}_r}^* + c_1 k'_3 \dot{u} \end{aligned} \tag{21}$$

Let $c_1 k_1'^2 \omega + c_1 k'_1 k'_2 + c_1 k'_1 k'_3 u - c_1{\ddot{\omega}_r}^* = \varphi$, $|\varphi| \le \delta, \delta \ge 0$

Using the super-twisting control algorithm and selecting the parameters of the super-twisting control law according to the method in (14), the system can be stabilized and converge in a limited time, finally $s = \dot{s} = 0$.

4.2. The Design of Fast Subsystem Control Law

The state variables of the fast subsystem shown in (18) do not have the expected output variables, so it only needs to be stable within a limited time for the fast subsystem. Since the state variable i_{qf} of the fast subsystem is not measurable, the design of the control law for the fast subsystem is a linear control law:

$$u_{qf} = -kx_f = -ki_{qf} \tag{22}$$

In (22), $k > 0$, put Equation (22) into Equation (18), the following equation can be obtained:

$$\dot{i}_{qf} = -(\frac{R_s + k}{\varepsilon}) i_{qf} \tag{23}$$

Because $-(R_s + k)/\varepsilon < 0$ and all of the eigenvalues of the fast system have negative real parts. The fast system is stable.

4.3. Compound Control

Add the control law of the fast subsystem and the slow subsystem, can obtain a compound control law:

$$u_q = u_{qs} + u_{qf} \tag{24}$$

For the PMSM servo system, the control laws of the slow subsystem and the fast subsystem are as follows:

$$\begin{aligned} u_{qs} &= -k_1 |s|^{1/2} \mathrm{sgn}(s) - \int k_2 \mathrm{sgn}(s) \\ u_{qf} &= -k i_{qf} = -k(i_q - i_{qs}) \end{aligned} \tag{25}$$

The slow-varying equation of current in (25) obtained by $\varepsilon \to 0$ is transformed into the equation of u_{qs}, Equation (25) can be equivalent to:

$$\begin{aligned} u_{qs} &= -k_1|s|^{1/2}\mathrm{sgn}(s) - \int k_2\mathrm{sgn}(s) \\ u_{qf} &= -k(i_q - \tfrac{u_{qs}}{R_s}) \end{aligned} \tag{26}$$

The schematic diagram of the second-order sliding mode control of the PMSM servo system based on the theory of singular perturbation is shown in Figure 3.

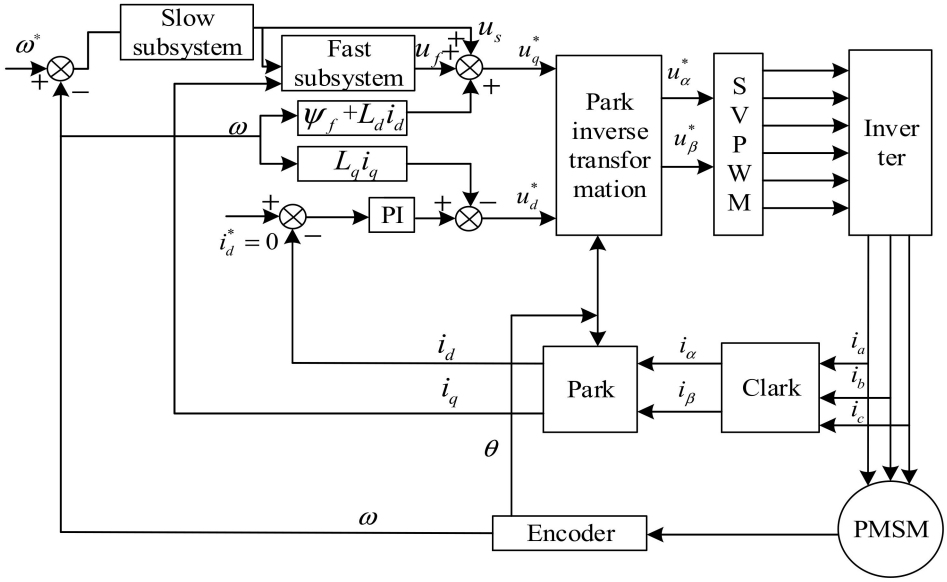

Figure 3. Schematic diagram of second-order sliding mode control of PMSM based on singular perturbation theory.

5. Experimental Verification

5.1. Experiment Platform

A PMSM experimental traction platform was built for verification. The schematic diagram of the experimental traction platform is shown in Figure 4, and the physical diagram of the traction experimental platform is shown in Figure 5. The power level of the PMSM is 1.5 kW. The parameters of the motor are shown in Table 1. The sampling frequency is set to 10 kHz.

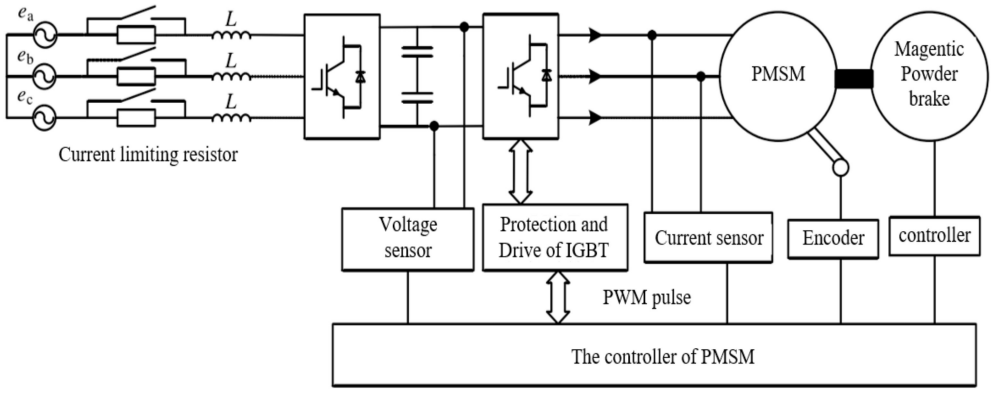

Figure 4. Structure of the PMSM traction experiment platform.

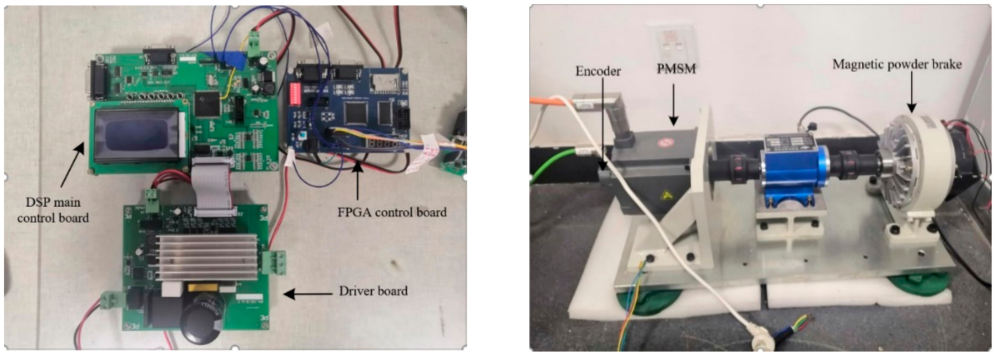

(**a**) (**b**)

Figure 5. Experiment platform of PMSM. (**a**) controllers and the main circuits. (**b**) permanent magnet synchronous motor.

Table 1. Experiment platform PMSM parameters.

System Parameter	Note	Value
Rated speed	N	2000 r/min
Rated voltage	U_{dc}	311 V
Pole-pairs number	n_p	4
Stator resistance	R_s	1.344 Ω
D-axis inductance	L_d	4.838 mH
Q-axis inductance	L_q	4.838 mH
Flux linkage	ψ_f	0.267 Wb
Rated power	P	1.5 kw

The experimental platform is mainly composed of three parts: the control circuit, the drive circuit, the motor, and the load device. The control circuit includes DSP, FPGA, and AD and DA chips. The model of the DSP used in the experiment is TMS320F28335. Because this model of DSP cannot meet the sampling frequency requirements of the encoder output signal, the PS21765 of the FPGA model is used as the auxiliary controller to decode the encoder signal and output the rotor position information to DSP. DSP as the core controller is responsible for executing the core algorithm and generating driving signals. The drive circuit is composed of a three-phase AC power supply, uncontrolled rectifier bridge, inverter, voltage, and current sensors. The AC power is converted to DC power by a rectifier, and the voltage and frequency of AC power are variable by means of the inverter. The load device controls the load by a magnetic powder brake.

5.2. Second-Order Sliding Mode Control

The key parameters of the SOSMC strategy are shown in Table 2. When the PMSM starts without load, the experimental result of the speed changes is shown in Figure 6 and Table 4. The motor starts with load, the speed is ramped to 500 r/min and keeps stable after 0.1 s, then the speed is reduced to 50 r/min and stabilizes after about 0.09 s. When the speed changes, the actual speed can quickly track the given value with almost no overshoot. The current value of the d-axis is zero, and the current value of the q-axis fluctuates slightly and quickly returns to a stable value when the speed changes. However, the current of the d-q axis has more harmonic noise components.

Table 2. The key parameters of the SOSMC strategy.

System Parameters	c_1	c_2	m_1	m_2	k_1	k_2
Symbol	150	1	1	600	8000	400

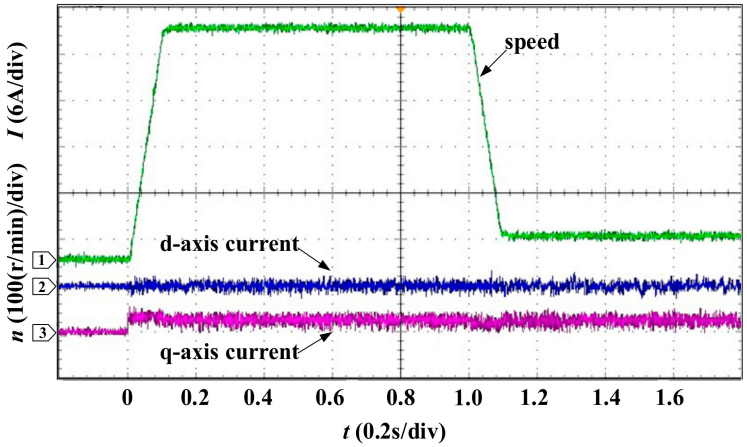

Figure 6. Experimental results of motor speed variation under second-order sliding mode control strategy.

When the load changes suddenly, the experimental results of PMSM based on the second-order sliding mode control strategy are shown in Figure 7 and Table 4. The motor starts with a load of 5 N·m. The given speed is 100 r/min and stabilizes after 0.01 s. The load is added to 10 N·m at 0.6 s, and all of the loads are removed at 1.2 s. In Figure 7, it can be found that the speed of the motor changes slightly when the load is suddenly added, and the load is reduced. In the whole process, the d-axis current always remains at zero, and the q-axis current changes slightly and quickly stabilize when the load changes. But the current of the d-q axis has more harmonic noise components.

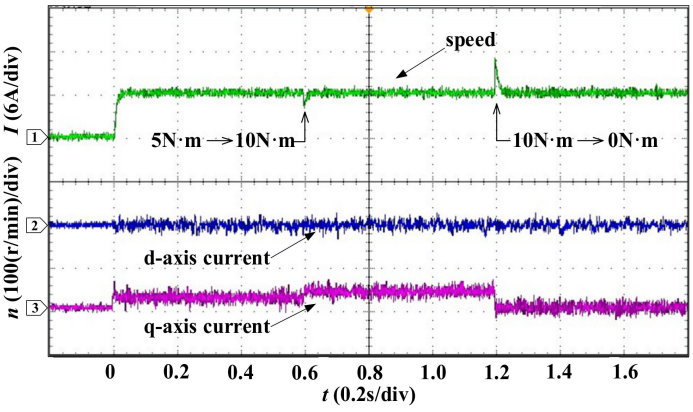

Figure 7. Experimental results of motor load variation under second-order sliding mode control strategy.

5.3. Second-Order Sliding Mode Control Based on Singular Perturbation

The key parameters of the SOSMC based on a singular perturbation strategy are shown in Table 3. When the speed changes, the experimental results of PMSM based on the singularly perturbed second-order sliding mode control strategy are shown in Figure 8 and Table 4. The motor starts with a load of 5 N·m, the speed is ramped to 500 r/min and stabilizes after 0.1 s, then the speed is reduced to 50 r/min and stabilizes after about 0.09 s. When the desired speed changes, the actual speed can quickly track the given value with almost no overshoot. The d-axis current is almost no fluctuation and always remains at zero. The q-axis current fluctuates slightly and quickly returns to a stable value when the speed changes. The process of the entire transition was smooth.

Table 3. The key parameters of the SOSMC based on singular perturbation strategy.

System Parameters	c_1	k_1	k_2	k
Symbol	10	0.5	100	180

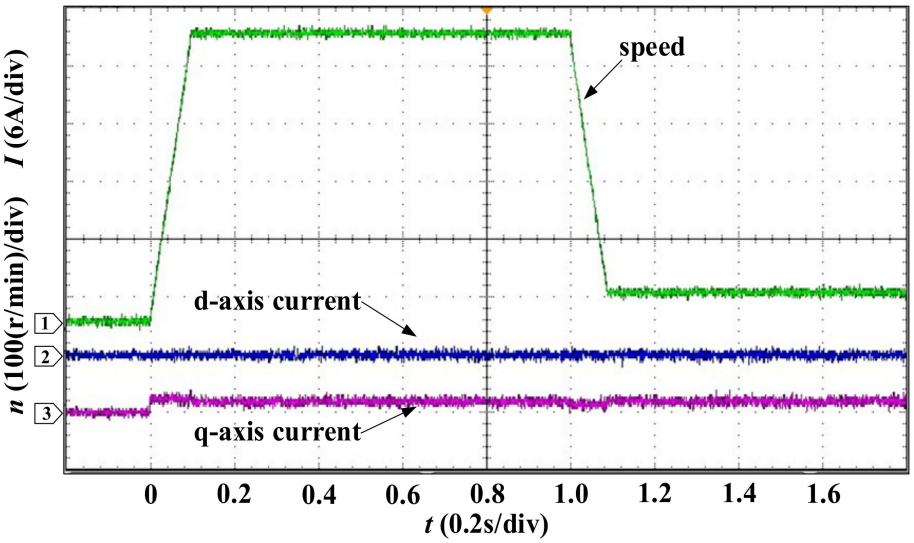

Figure 8. Experimental results of motor speed variation based on second-order sliding mode control with singular perturbation.

Table 4. PMSM system performance.

Result	SOSMC	SOSMC Based on Singular Perturbation
Response Time (Accelerate)	0.1	0.1
Response Time (Deceleration)	0.09	0.09
Response10 N·m)	0.04	0.02
Response5 N·m)	0.04	0.02
Speed10 N·m)	30	20
Speed5 N·m)	90	40
$i_q^{rip}(A)$	2.4	1.2

When the load changes suddenly, the experimental results of PMSM based on the singularly perturbed second-order sliding mode control strategy are shown in Figure 9. The motor starts with a load of 5 N·m. The speed is ramped to 500 r/min and keeps stable, then the load is added to 10 N·m, and the load is removed after it stabilizes again. In Figure 9 and Table 4, it can be found that when the load is added, or the load is suddenly reduced, the motor speed changes almost slightly and quickly returns to the given value. In the whole process, the d-axis current has almost no fluctuations and remains at zero. The q-axis current changes slightly and stabilizes in a very short time when the load changes. It shows that the system has strong robustness and good anti-load disturbance ability based on this strategy.

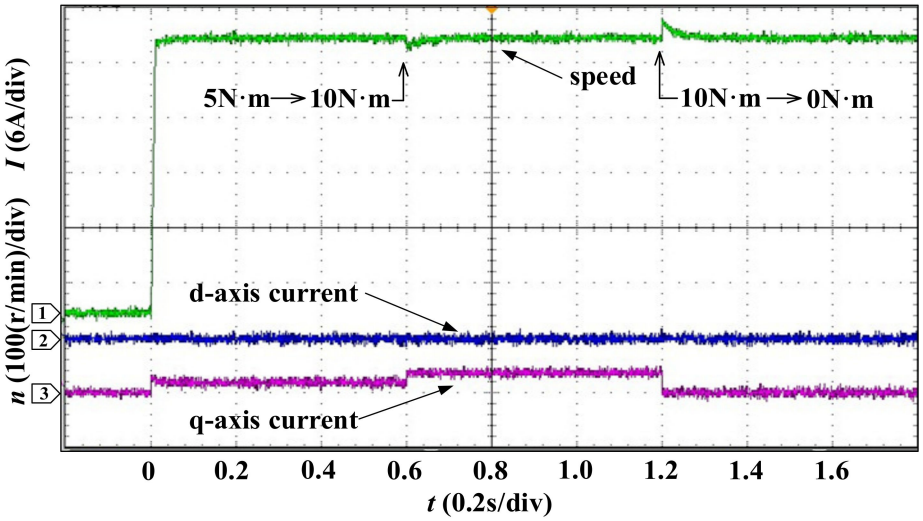

Figure 9. Experimental results of motor load variation based on singular perturbation second-order sliding mode control strategy.

6. Conclusions

This study proposes a second-order sliding-mode controller based on singular perturbation based on second-order sliding-mode control. The method is applied to motor control, solving the jitter problem in conventional sliding mode control and simplifying the controller design process compared to second-order superhelix sliding mode control.

The design of the sliding surface is simplified by decomposing the original system down to a lower order using the singular ingestion method. In addition, the design of the robust differentiator is optimized, thereby eliminating high-frequency noise. Experimental results show that the proposed method outperforms the second-order sliding mode control in terms of robustness in the face of sudden load addition and reduction and steady-state performance in steady operation. This demonstrates the excellent dynamic steady-state performance of the proposed method while simplifying the controller design.

Author Contributions: Conceptualization, Y.H.; Data curation, B.L. and Q.W.; Funding acquisition, T.G.; Methodology, Y.H.; Software, Z.L.; Supervision, T.G.; Validation, Q.W.; Writing–original draft, Z.L.; Writing–review & editing, B.L. All authors have read and agreed to the published version of the manuscript.

Funding: This research work was funded by [2022 Jiangsu Provincial Postgraduate Research & Practice Innovation Program] grant number [SJCX22_1168]. This research work was funded by [Graduate Innovation Program of China University of Mining and Technology] grant number [2022WLJCRCZL337].

Data Availability Statement: The data supporting the findings of this study are available within the article.

Conflicts of Interest: The authors declare no conflict of interest.

References

1. Choi, H.H.; Vu, N.T.-T.; Jung, J.-W. Digital Implementation of an Adaptive Speed Regulator for a PMSM. *IEEE Trans. Power Electron.* **2011**, *26*, 3–8. [CrossRef]
2. Rahul, D.; Anwar, M.N. Design of fractional order PI controller for first order plus dead time process based on maximum sensitivity. In Proceedings of the 2018 2nd International Conference on Energy, Power and Environment(ICEPE), Shanghai, China, 1–2 June 2018; pp. 1–6.
3. Nam, S.; Son, J.E.; Kim, N. Real-time air conditioner zone temperature control by cascaded intelligent PI. In Proceedings of the 2017 17th International Conference on Control, Automation and Systems (ICCAS), Jeju, Korea, 18–21 October 2017; pp. 732–735.
4. Zhou, G.; Shi, X.; Fu, C.; Wang, Y. Operation of a Three-phase Soft Phase Locked Loop Under Distorted Voltage Conditions Using Intelligent PI Controller. In Proceedings of the 2006 IEEE Region 10 Conference, Hong Kong, China, 14–17 November 2016; pp. 1–4.

5. Yang, C.; Qin, R.; Tao, H.; Chen, Z.; Yang, C.; Peng, T. A Tracking Method of Load Current Based on Finite Set Model Predictive Control for Motor Simulator. In Proceedings of the 2018 International Conference on Intelligent Rail Transportation (ICIRT) Sands Expo and Convention Centre, Singapore, 12–14 December 2018; pp. 1–5.
6. Huo, Z.; Wang, B.; Yu, Y.; Wang, T.; Luo, C.; Xu, D. An Extended Speed Adaptive Observer with Auxiliary Variables for Sensorless Induction Motor Low-Speed Operation. In Proceedings of the 22nd International Conference on Electrical Machines and Systems (ICEMS), Harbin, China, 11–14 August 2019; pp. 1–4.
7. Jia, L.; Huang, Y.; Zheng, J.; Chen, J.; Tao, Y.; Li, P. Fuzzy Sliding Mode Control of Permanent Magnet Synchronous Motor Based on the Integral Sliding Mode Surface. In Proceedings of the 22nd International Conference on Electrical Machines and Systems (ICEMS), Harbin, China, 11–14 August 2019; pp. 6–11.
8. Wang, Y.; Xia, Y.; Li, H.; Zhou, P. A new integral sliding mode design method for nonlinear stochastic systems. *Automatica* **2018**, *90*, 304–309. [CrossRef]
9. Wang, Y.; Gao, Y.; Karimi, H.R.; She, H.; Fang, Z. Sliding Mode Control of Fuzzy Singularly Perturbed Systems With Application to Electric Circuit. *IEEE Trans. Syst. Man Cybern. Syst.* **2018**, *48*, 1667–1675. [CrossRef]
10. Wasu, S.M.; Sarode, U.B.; Bhavalkar, M.P. Speed control of PMSM system using improved reaching law based sliding mode control and disturbance observer technique. *Int. J. Adv. Comput. Res.* **2013**, *3*, 312–318.
11. Sun, G.; Ma, Z.; Yu, J. Discrete-time fractional order terminal sliding mode tracking control for linear motor. *IEEE Trans. Ind. Electron.* **2018**, *65*, 3386–3394. [CrossRef]
12. Van, M.; Mavrovouniotis, M.; Ge, S.S. An Adaptive Back stepping Nonsingular Fast Terminal Sliding Mode Control for Robust Fault Tolerant Control of Robot Manipulators. *IEEE Trans. Syst.* **2019**, *49*, 1448–1459.
13. Wang, Y.; Feng, Y.; Zhang, X.; Liang, J. A New Reaching Law for Antidisturbance Sliding-Mode Control of PMSM Speed Regulation System. *IEEE Trans. Power Electron.* **2020**, *35*, 4117–4127. [CrossRef]
14. Zhang, B.; Li, Y. A PMSM Sliding Mode Control System Based on Model Reference Adaptive Control. In Proceedings of the International Power Electronics & Motion Control Conference, Beijing, China, 15–18 August 2000; pp. 336–341.
15. Liang, D.; Li, J.; Qu, R.; Kong, W. Adaptive Second-Order Sliding-Mode Observer for PMSM Sensorless Control Considering VSI Nonlinearity. *IEEE Trans. Power Electron.* **2017**, *33*, 8994–9004. [CrossRef]
16. Zhao, K.; Yin, T.; Zhang, C.; He, J.; Li, X.; Chen, Y.; Zhou, R.; Leng, A. Robust Model-Free Nonsingular Terminal Sliding Mode Control for PMSM Demagnetization Fault. *IEEE Access* **2019**, *7*, 15737–15748. [CrossRef]
17. Qi, L.; Shi, H. A Novel Second Order Sliding Mode Control Algorithm for Velocity Control Permanent Magnet Synchronous Motor. In Proceedings of the International Conference on Intelligent Computing for Sustainable Energy and Environment(ICSEE), Shanghai, China, 12–13 September 2012; pp. 213–220.
18. Mohamadian, M.; Pedram, M.; Ashrafzadeh, F. Digital second order sliding mode control for a synchronous reluctance motor. In Proceedings of the 39th IAS Annual Meeting, Seattle, WA, USA, 3–7 October 2004; Volume 3, pp. 1899–1902.
19. Zhang, B.; Pi, Y. Hybrid first and second order sliding mode control for permanent magnet synchronous motor. In Proceedings of the IEEE/ASME International Conference on Advanced Intelligent Mechatronics, Kaohsiung, Taiwan, 11–14 July 2012; pp. 1000–1004.
20. Laghrouche, S.; Plestan, F.; Glumineau, A.; Boisliveau, R. Robust second order sliding mode control for a permanent magnet synchronous motor. In Proceedings of the American Control Conference, Denver, CO, USA, 4–6 June 2003; Volume 5, pp. 4071–4076.
21. Mu, C.; Xu, W.; Yu, X.; Sun, C. A continuous sliding mode controller for the PMSM speed regulation based on disturbance observer. In Proceedings of the 40th Annual Conference of the IEEE Industrial Electronics Society, Dallas, TX, USA, 29 October –1 November 2014; pp. 28–33.
22. Scalcon, F.P.; Fang, G.; Vieira, R.P.; Grundling, H.A.; Emadi, A. Discrete-Time Super-Twisting Sliding Mode Current Controller with Fixed Switching Frequency for Switched Reluctance Motors. *IEEE Trans. Power Electron.* **2022**, *37*, 3321–3333. [CrossRef]
23. Gao, P.; Zhang, G.; Lv, X. Model-free control using improved smoothing extended state observer and super-twisting nonlinear sliding mode control for PMSM drives. *Energies* **2021**, *14*, 922. [CrossRef]
24. Liu, Y.C.; Laghrouche, S.; N'Diaye, A.; Cirrincione, M. Hermite neural network-based second-order sliding-mode control of synchronous reluctance motor drive systems. *J. Frankl. Inst.* **2021**, *358*, 400–427. [CrossRef]